Perturbation Finite Element Method for Magnetostatic and Magnetodynamic Problems

Patrick Dular, Ruth V. Sabariego, Laurent Krähenbühl

Perturbation Finite Element Method for Magnetostatic and Magnetodynamic Problems

Patrick Dular[1,2], Ruth V. Sabariego[1] and Laurent Krähenbühl[3]
[1] Dept. of Electrical Engineering and Computer Science, ACE, [2]FNRS, University of Liège, B28, B-4000 Liège, Belgium
[3] Université de Lyon, Ampère (UMR CNRS 5005), École Centrale de Lyon, F-69134 Écully Cedex, France

***Abstract*—Magnetic flux distributions are calculated in magnetostatic and magnetodynamic problems via a subproblem finite element method based on a perturbation technique. An approximate finite element problem considering ideal flux tubes or ideal materials is first solved. It gives the source for finite element perturbation problems considering the flux tubes with their exterior regions, accounting thus for leakage fluxes, as well as for changes of material properties and shapes. The proposed technique aims to accurately quantify the gain given by each model refinement on both local fields and global quantities and to justify the usefulness of this refinement. It is also well adapted to parameterized analyses on geometrical and material data.**

***Index Terms* — Finite element method, magnetostatic, magnetodynamic, perturbation method.**

I. INTRODUCTION

The perturbation of finite element (FE) solutions provides clear advantages in repetitive analyses [1]-[5] and helps improving the solution accuracy [6]-[9]. This technique allows to benefit from previous computations instead of starting a new complete FE solution for any variation of geometrical or physical data. It also allows different problem-adapted meshes and increases computational efficiency thanks to the reduced size of each subproblem.

A perturbation FE method is herein developed for accurately calculating the magnetic flux distribution and all the ensuing quantities in magnetostatic and magnetodynamic problems starting from approximate solutions. An approximate problem is first solved via a simplified FE analysis, considering simplified models, e.g. ideal flux tubes, ideal materials or simplified geometries. Perturbation problems consider then some modifications towards real materials and field supports, which result in changes in flux distributions, e.g. allowing leakage flux or field penetration. From the so calculated field corrections, the associate corrections of global quantities, i.e. fluxes and magnetomotive forces (MMFs), voltage and currents, are also evaluated to determine reluctances [10] and impedances [11]. The method also allows to build accurate reluctance networks, possibly starting from preliminary approximations [12]. Each problem is defined in its own domain with an adapted and distinct mesh refinement. The developments are performed for the magnetic vector potential FE magnetostatic and magnetodynamic formulations, paying special attention to the proper discretization of the source constraints. The method is applied to several problems to point out its main characteristics and advantages.

P. Dular, Patrick.Dular@ulg.ac.be, R.V. Sabariego, R.Sabariego@ulg.ac.be, L. Krähenbühl, Laurent.Krahenbuhl@ec-lyon.fr

This work was supported by F.R.S.-FNRS, the Belgian Science Policy (IAP P6/21) and the Belgian French Community (Research Concerted Action ARC 03/08-298).

II. FORMULATION OF A CANONICAL PROBLEM

A. Canonical problem with volume and surface sources

A canonical magnetodynamic problem p is defined in a domain Ω_p, with boundary $\partial\Omega_p=\Gamma_p=\Gamma_{h,p}\cup\Gamma_{b,p}$ (possibly at infinity). The eddy current conducting part of Ω_p is denoted $\Omega_{c,p}$ and the non-conducting one $\Omega_{c,p}{}^C$, with $\Omega_p=\Omega_{c,p}\cup\Omega_{c,p}{}^C$. Massive inductors belong to $\Omega_{c,p}$, whereas stranded inductors belong to $\Omega_{c,p}{}^C$. Subscript p refers to the associated problem p. The equations, material relations, boundary conditions (BCs) and interface conditions (ICs) of problem p are

$$\operatorname{curl}\boldsymbol{h}_p=\boldsymbol{j}_p\,,\quad \operatorname{curl}\boldsymbol{e}_p=-\partial_t\boldsymbol{b}_p\,,\quad \operatorname{div}\boldsymbol{b}_p=0\,, \qquad \text{(1a-b-c)}$$

$$\boldsymbol{b}_p=\mu_p\,\boldsymbol{h}_p+\boldsymbol{b}_{s,p}\,,\quad \boldsymbol{j}_p=\sigma_p\,\boldsymbol{e}_p+\boldsymbol{j}_{s,p}\,, \qquad \text{(1d-e)}$$

$$\boldsymbol{n}\times\boldsymbol{h}_p|_{\Gamma_{h,p}}=0\,,\ \boldsymbol{n}\times\boldsymbol{e}_p|_{\Gamma_{e,p}\subset\Gamma_{b,p}}=0\,,\ \boldsymbol{n}\cdot\boldsymbol{b}_p|_{\Gamma_{b,p}}=0\,, \qquad \text{(1f-g-h)}$$

$$[\boldsymbol{n}\times\boldsymbol{h}_p]_{\gamma_p}=\boldsymbol{j}_{su,p},\ [\boldsymbol{n}\times\boldsymbol{e}_p]_{\gamma_p}=\boldsymbol{k}_{su,p},\ [\boldsymbol{n}\cdot\boldsymbol{b}_p]_{\gamma_p}=\boldsymbol{b}_{su,p}, \qquad \text{(1i-j-k)}$$

where $\boldsymbol{h}_p$ is the magnetic field, $\boldsymbol{b}_p$ is the magnetic flux density, $\boldsymbol{e}_p$ is the electric field, $\boldsymbol{j}_p$ is the electric current density (including source and eddy currents), μ_p is the magnetic permeability, σ_p is the electric conductivity and $\boldsymbol{n}$ is the unit normal exterior to Ω_p. Note that (1b) is only defined in $\Omega_{c,p}$ (as $\boldsymbol{e}_p$), whereas it is reduced to the form (1c) in $\Omega_{c,p}{}^C$. It is thus absent from the magnetostatic version of problem (1a-k). Further (1g) is more restrictive than (1h).

The fields $\boldsymbol{b}_{s,p}$ and $\boldsymbol{j}_{s,p}$ are volume sources. The source $\boldsymbol{b}_{s,p}$ is usually used for fixing a remnant induction in magnetic materials. The source $\boldsymbol{j}_{s,p}$ usually fixes the current density in stranded inductors. These sources are further generalized to account for other constraints.

The notation $[\,\cdot\,]_\gamma=\cdot\,|_{\gamma^+}-\cdot\,|_{\gamma^-}$ expresses the discontinuity of a quantity through any interface γ (with sides γ^+ and γ^-) in Ω_p (the region in between is considered to be exterior to Ω_p). The associated surface fields $\boldsymbol{j}_{su,p}$, $\boldsymbol{k}_{su,p}$ and $\boldsymbol{b}_{su,p}$ are generally zero, defining classical ICs for the physical fields, i.e. the continuities of the tangential component of $\boldsymbol{h}_p$ and $\boldsymbol{e}_p$ and of the normal component of $\boldsymbol{b}_p$. If nonzero, they define possible surface sources that account for particular phenomena occurring in the idealized thin region between γ^+ and γ^-.

Each problem p is to be constrained via the so-defined volume and surface sources from parts of the solution of other problems. This is a key of the developed method.

B. b-conform magnetic vector potential weak formulation

The canonical problem p (1a-k) is defined in Ω_p with the magnetic vector potential formulation [11], expressing the magnetic flux density $\boldsymbol{b}_p$ in Ω_p as the curl of a magnetic vector potential $\boldsymbol{a}_p$, and the electric field $\boldsymbol{e}_p$ in $\Omega_{c,p}$ as $\boldsymbol{e}_p=-\partial_t\boldsymbol{a}_p$. The related $\boldsymbol{a}$-formulation is obtained from the weak form of the Ampère equation (1a), i.e. [11],

$$
\begin{aligned}
&(\mu_p^{-1}\,\mathrm{curl}\,\boldsymbol{a}_p,\mathrm{curl}\,\boldsymbol{a}')_{\Omega_p}-(\boldsymbol{h}_{s,p},\mathrm{curl}\,\boldsymbol{a}')_{\Omega_p}\\
&+(\sigma_p\,\partial_t\boldsymbol{a}_p,\boldsymbol{a}')_{\Omega_{c,p}}-(\boldsymbol{j}_{s,p},\boldsymbol{a}')_{\Omega_{s,p}\subset\Omega_p}\\
&+<\boldsymbol{n}\times\boldsymbol{h}_{s,p},\boldsymbol{a}'>_{\Gamma_{h,p}}+<\boldsymbol{n}\times\boldsymbol{h}_p,\boldsymbol{a}'>_{\Gamma_{b,p}}\\
&+<[\boldsymbol{n}\times\boldsymbol{h}_p]_{\gamma_p},\boldsymbol{a}'>_{\gamma_p}=0\ ,\quad \forall\,\boldsymbol{a}'\in F_p{}^1(\Omega_p)\,, \qquad (2)
\end{aligned}
$$

where $F_p{}^1(\Omega_p)$ is a gauged curl-conform function space defined on Ω_p and containing the basis functions for $\boldsymbol{a}$ as well as for the test function $\boldsymbol{a}'$ (at the discrete level, this space is defined by edge FEs); $(\cdot\,,\cdot)_\Omega$ and $<\cdot\,,\cdot>_\Gamma$ respectively denote a volume integral in Ω and a surface integral on Γ of the product of their vector field arguments. A major consequence of the ***b***-conform formulation used is that ICs (1i) and (1k) are defined respectively in strong and weak senses (essential and natural ICs), i.e. in $F_p{}^1(\Omega_p)$ and via a surface integral term. The surface integral term on $\Gamma_{h,p}$ accounts for natural BCs of type (1f), usually with $\boldsymbol{n}\times\boldsymbol{h}_{s,p}|_{\Gamma_{h,p}}=0$. The unknown term on the surface $\Gamma_{b,p}$ with essential BCs on $\boldsymbol{n}\cdot\boldsymbol{b}_p$ is usually omitted because it does not locally contribute to (2). It will be shown to be the key for the post-processing of a solution p, a part of which, $\boldsymbol{n}\times\boldsymbol{h}_p|_{\Gamma_{b,p}}$, is used as a source in further problems.

C. Projections of solutions between meshes

Some parts of a previous solution $\boldsymbol{a}_q$ are intended to serve as sources in a subdomain $\Omega_{s,p}\subset\Omega_p$ of the current problem p. At the discrete level, this means that this source quantity $\boldsymbol{a}_q$ has to be expressed in the mesh of problem p, while initially given in the mesh of problem q. This can be done via a projection method [13] of its curl limited to $\Omega_{s,p}$, i.e.

$$
\begin{aligned}
&(\mathrm{curl}\,\boldsymbol{a}_q^{p\text{-}proj},\mathrm{curl}\,\boldsymbol{a}')_{\Omega_{s,p}}=(\mathrm{curl}\,\boldsymbol{a}_q,\mathrm{curl}\,\boldsymbol{a}')_{\Omega_{s,p}}\,,\\
&\qquad\forall\,\boldsymbol{a}'\in F_p{}^1(\Omega_{s,p})\,, \qquad (3)
\end{aligned}
$$

where $F_p{}^1(\Omega_{s,p})$ is a gauged curl-conform function space for the p-projected source $\boldsymbol{a}_q^{p\text{-}proj}$ (the projection of $\boldsymbol{a}_q$ on mesh p) and the test function $\boldsymbol{a}'$. Directly projecting $\boldsymbol{a}_q$ (not its curl) would result in numerical inaccuracies when evaluating its curl.

III. A Series of Perturbation Subproblems

A. Sequence of perturbation subproblems

The solution $\boldsymbol{u}$ of a complete problem is expressed as the sum of subproblem solutions $\mathbf{u}_p$. It is generally worth defining an appropriate series of subproblems via successive model refinements of an initially simplified model. Physical considerations help in building such a series. For the associated ordered set P of subproblems, the complete solution is then

$$
\boldsymbol{u}=\sum\nolimits_{p\in P}\boldsymbol{u}_p\ ,\ \text{with}\ \boldsymbol{u}\equiv\boldsymbol{h},\boldsymbol{b},\boldsymbol{j}_{su},\boldsymbol{b}_{su},... \qquad (4)
$$

Each subproblem is defined in its own domain, possibly distinct from the complete domain. Constraints and relations are thus not necessarily shared with the complete problem. At the discrete level, this decreases the problem complexity and allows distinct meshes with suitable refinements.

As a consequence, each subproblem is generally perturbed by all the others and each solution $\mathbf{u}_p$ has to be calculated as a series of corrections or perturbations $\mathbf{u}_{p,i}$, i.e.

$$
\boldsymbol{u}_p=\sum\nolimits_i\boldsymbol{u}_{p,i}=\boldsymbol{u}_{p,1}+\boldsymbol{u}_{p,2}+... \qquad (5)
$$

The calculation of the correction $\mathbf{u}_{p,i}$ in a subproblem p,i (problem p with particular constraints at iteration i) is kept on till convergence up to a desired accuracy. For well posed problems, the corrections tend to zero with the iterations. Each correction must account for the influence of all the previous corrections $\mathbf{u}_{p,j}$ of the other subproblems, with j the last iteration index for which a correction is known. This way, once some corrections have acted as sources for solutions $\mathbf{u}_{p,i}$, they are skipped in the next subproblems p,k, with $k>i$. Initial solutions $\mathbf{u}_{p,0}$ are set to zero. The iterative process is required when a correction becomes a significant source for any of its source problems, which is inherent to large perturbation problems. In addition to the iterations between subproblems, classical inter-problem iterations are needed in nonlinear analyses. The global quantities linearly related to each correction, i.e. the fluxes and MMFs [10], or the voltages and currents [11], are added to obtain their complete values. Obviously, the more accurate model ensures a gain in precision.

B. Possible approximations in subproblems

A subproblem p can disregard some materials initially present in previous subproblems q, while these exist in the complete problem. At the discrete level, this generally allows to reduce the meshing efforts and the computational cost of the solution p. In particular, any intersection of the non-material regions of Ω_p with the material regions of Ω_q is allowed [2], [5]. The defined iterative process between all problems will correct their interactions.

IV. Perturbations via Volume Sources

A. Change of material properties

A change of a material property in a volume region, due to either the change of properties of existing materials or the addition/suppression of materials (connected or not to already existing ones), generates a volume source (or a region-type source) in the associated material relation. For a change of permeability, from μ_q for problem q to μ_p for problem p, the volume source in the ***b*-*h*** relation (1d) is of the form

$$
\boldsymbol{b}_{s,p}=(\mu_p-\mu_q)\,\boldsymbol{h}_q\,. \qquad (6)
$$

Summing both subproblem relations $\boldsymbol{b}_q=\mu_q\boldsymbol{h}_q$ (with e.g. $\boldsymbol{b}_{s,q}=0$) and $\boldsymbol{b}_p=\mu_p\boldsymbol{h}_p+\boldsymbol{b}_{s,p}$ gives the relation that is valid for the superposition of solutions q and p, i.e. $\boldsymbol{b}_q+\boldsymbol{b}_p=\mu_q\boldsymbol{h}_q+\mu_p\boldsymbol{h}_p+(\mu_p-\mu_q)\boldsymbol{h}_q=\mu_p(\boldsymbol{h}_q+\boldsymbol{h}_p)$. Analogously, the ***h*-*b*** relation would be

$$
\boldsymbol{h}_p=\mu_p{}^{-1}\boldsymbol{b}_p+\boldsymbol{h}_{s,p}\ ,\ \text{with}\ \boldsymbol{h}_{s,p}=(\mu_p{}^{-1}-\mu_q{}^{-1})\boldsymbol{b}_q\,. \qquad (7a\text{-}b)
$$

Also, for a change of conductivity, from σ_q for problem q to σ_p for problem p, the volume source in the ***j*-*e*** relation (1e) is of the form

$$
\boldsymbol{j}_{s,p}=(\sigma_p-\sigma_q)\,\boldsymbol{e}_q\,. \qquad (8)
$$

The generalization of (6) and (8) to an arbitrary number of source subproblems gives

$$
\boldsymbol{b}_{s,p}=(\mu_p-\mu_q)\sum\nolimits_{r\in P,r\neq p}\boldsymbol{h}_r\ , \qquad (9)
$$

$$
\boldsymbol{j}_{s,p}=(\sigma_p-\sigma_q)\sum\nolimits_{r\in P,r\neq p}\boldsymbol{e}_r\ , \qquad (10)
$$

with q the last solved problem.

B. *Possible approximations*

As already introduced approximations, the sources $\boldsymbol{b}_{s,p}$ or $\boldsymbol{j}_{s,p}$ can be neglected in some regions, although μ_p and μ_q, or σ_p and σ_q, may differ. This amounts to disregard these regions and avoid their meshing. The ***b*-*h*** material relation for the complete fields in these regions is thus

$$\boldsymbol{b}_q + \boldsymbol{b}_p = \mu_q \boldsymbol{h}_q + \mu_p \boldsymbol{h}_p \,, \tag{11}$$

that can be transformed, with (4), as

$$\boldsymbol{b} = \mu_q \boldsymbol{h} + (\mu_p - \mu_q)\, \boldsymbol{h}_p \,. \tag{12}$$

When the material properties differ too much between states q and p, and the perturbation fields are too large compared to the source fields, the last term in (12) is not negligible and the error is clearly highlighted. The correct relation, $\boldsymbol{b} = \mu_p \boldsymbol{h}$, is only rigorously fulfilled in the regions where μ does not vary ($\mu_p = \mu_q$). An analogous approximation applies for the ***j*-*e*** relation.

C. *Volume source in weak formulation*

A change of material properties from problem q to p is taken into account via volume integrals in the weak formulation (2). A change from μ_q to μ_p is defined via the integral $(\boldsymbol{h}_{s,p}, \mathrm{curl}\, \boldsymbol{a}')_{\Omega_p}$. The volume source $\boldsymbol{h}_{s,p}$ is given by (7b), i.e. $\boldsymbol{h}_{s,p} = (\mu_p^{-1} - \mu_q^{-1})\boldsymbol{b}_q$, with $\boldsymbol{b}_q = \mathrm{curl}\, \boldsymbol{a}_q$. At the discrete level, the source primal quantity $\boldsymbol{a}_q$ in mesh q is projected in mesh p via (3), with $\Omega_{s,p}$ limited to the modified regions. A change of current density in either added or modified inductors is defined in (2) via the source integral $(\boldsymbol{j}_{s,p}, \boldsymbol{a}')_{\Omega_p}$ with the associated volume source $\boldsymbol{j}_{s,p}$. In particular, volume inductors can be defined in place of preliminary surface idealized inductors of ideal flux tubes. The source integral occurs also with a change of conductivity from σ_q to σ_p, with the source $\boldsymbol{j}_{s,p}$ given by (8).

As a first illustration, a sequence of problems considers a solution 1 with preliminary dimensions of an I-core, followed by the correction for its elongation (addition of a material region) (Figs. 1 and 2) [9]. Because the correction is only significant in the vicinity of the added region, the domain and mesh required for its calculation can be reduced (with appropriate BC, $\boldsymbol{n} \times \boldsymbol{h}_2|_{\Gamma_{h,2}} = 0$, on the core sections included in $\Gamma_{h,2}$). The I-core end effect of solution 1 is properly corrected, i.e. shifted and reduced at the new end. The initial inductor flux linkage is $\Phi_1 = 144.3$ mWb and its correction is $\Phi_2 = 3.5$ mWb (relative correction 2.4 %).

Another sequence of problems starts with the preliminary system and corrects it for a change of permeability of the I-core ($\mu_{r,I\text{-}core,1} = 500$, $\mu_{r,I\text{-}core,2} = 100$) (Fig. 3) [9]. An accurate correction is also obtained. The initial inductor flux linkage is $\Phi_1 = 144.3$ mWb and its correction is $\Phi_2 = -19.3$ mWb (relative correction 13.4 %).

An inductor core system (Fig. 4) is then considered (core with surrounding coil, frequency 50 Hz, relative permeability $\mu_{r,\,core} = 100$) [2]. A perturbing conductive region $\Omega_{c,2}$ is a rectangular plate, defining a change from $\sigma_1 = 0$ to $\sigma_2 \neq 0$. Eddy currents in the plate, as well as the impedance change of the coil, can be efficiently calculated for various positions of the plate without remeshing the exterior air region. This strongly simplifies the treatment of moving systems (Fig. 5) [5]. Other perturbation problems, with changes from $\sigma_1 \neq 0$ to $\sigma_2 = 0$, can be used in non-destructive eddy current testing for crack detection [1], [3], [4].

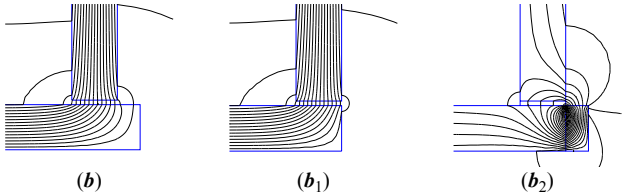

Fig. 1. Field lines of the complete solution ($\boldsymbol{b}$), sum of the initial I-core solution ($\boldsymbol{b}_1$) and perturbation elongated I-core solution ($\boldsymbol{b}_2$) [9].

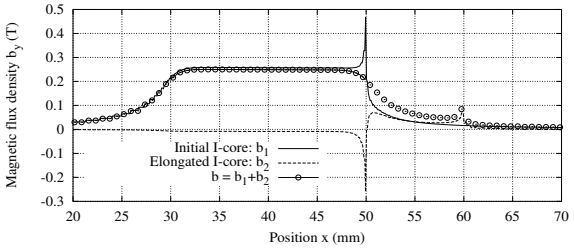

Fig. 2. Magnetic flux density along the top surface of the I-core entering the air gap for the initial I-core ($\boldsymbol{b}_1$) and its elongation perturbation ($\boldsymbol{b}_2$) [9].

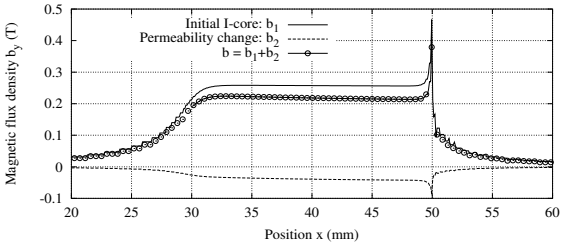

Fig. 3. Magnetic flux density along the top surface of the I-core entering the air gap for the initial I-core ($\boldsymbol{b}_1$) and for the permeability change ($\boldsymbol{b}_2$) [9].

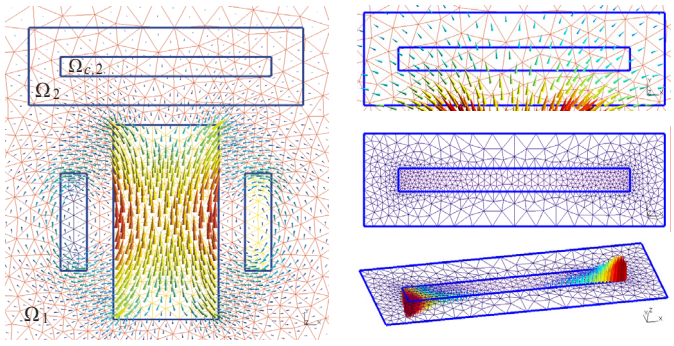

Fig. 4. Problems 1 (*left:* mesh of Ω_1 and distribution of $\boldsymbol{b}_1$) and 2 (*top right:* $\boldsymbol{b}_1$ to be projected in $\Omega_{c,2}$ for the volume source; *middle right:* adapted mesh of Ω_2; *bottom right:* $\boldsymbol{j}_2$ in $\Omega_{c,2}$) [2].

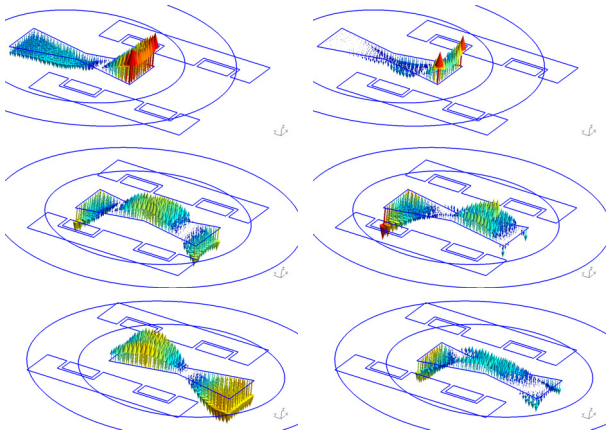

Fig. 5. Source electric field $\boldsymbol{e}_1$ (*left*) and perturbation current density $\boldsymbol{j}_2$ in $\Omega_{c,2}$ (*right*); for different positions of the moving piece [5].

V. Perturbations via Surface Sources

A. Changes of ICs – general considerations

For a first problem $p=1$, ICs through an interface γ_1 can be first defined to limit the support of the field solution on one side of γ_1, i.e. in the domain Ω_1^+ bordered by γ_1^+. This allows a preliminary reduction of the studied domain and applies e.g. to ideal flux tubes and perfect conductive or magnetic materials, as detailed hereafter. The traces of the fields on γ_1^+ can be either known or unknown, while there are zeroed on γ_1^- to account for zero fields in the bordered domain Ω_1^-, i.e.

$$\boldsymbol{n}\cdot\boldsymbol{b}_1|_{\gamma_1^+}=\boldsymbol{b}_{su,1}\,,\quad \boldsymbol{n}\cdot\boldsymbol{b}_1|_{\gamma_1^-}=0\,, \tag{13a-b}$$

$$\boldsymbol{n}\times\boldsymbol{h}_1|_{\gamma_1^+}=\boldsymbol{j}_{su,1}\,,\quad \boldsymbol{n}\times\boldsymbol{h}_1|_{\gamma_1^-}=0\,, \tag{14a-b}$$

or, for the discontinuities or ICs through γ_1,

$$[\boldsymbol{n}\cdot\boldsymbol{b}_1]_{\gamma_1}=\boldsymbol{b}_{su,1}\,,\quad [\boldsymbol{n}\times\boldsymbol{h}_1]_{\gamma_1}=\boldsymbol{j}_{su,1}\,. \tag{15a-b}$$

Problem 2 must correct the solution 1 via appropriate ICs (1 i) and (1k). On the one hand,

$$[\boldsymbol{n}\cdot\boldsymbol{b}_2]_{\gamma_2}=\boldsymbol{b}_{su,2}=[\boldsymbol{n}\cdot\boldsymbol{b}]_{\gamma_2}-\boldsymbol{b}_{su,1}=-\boldsymbol{n}\cdot\boldsymbol{b}_1|_{\gamma_1^+}\,, \tag{16}$$

due to the actual continuity of $\boldsymbol{n}\cdot\boldsymbol{b}$ in the complete solution (4) and with the trace $\boldsymbol{b}_{su,1}$ given by (13a). On the other hand,

$$[\boldsymbol{n}\times\boldsymbol{h}_2]_{\gamma_2}=\boldsymbol{j}_{su,2}=[\boldsymbol{n}\times\boldsymbol{h}]_{\gamma_2}-\boldsymbol{j}_{su,1}=-\boldsymbol{n}\times\boldsymbol{h}_1|_{\gamma_1^+}\,, \tag{17}$$

due to the actual continuity of $\boldsymbol{n}\times\boldsymbol{h}$ in the complete solution (4) and relation (14a). Problem 2 not only extends the solution in the domain bordered by γ_2^-, but also corrects it in the domain bordered by γ_2^+. Note that γ_1 and γ_2 are equivalent. They only differ at the discrete level due to their different meshes.

ICs of types (16) and (17) are surface sources (or interface-type sources) fixing the trace discontinuities of $\boldsymbol{h}_p$ and $\boldsymbol{b}_p$ in terms of other solutions q. The forced discontinuities introduced in a problem can thus be corrected by another one. The constraints of each problem, when defined in the $\boldsymbol{b}$-conform formulation (2), are of essential or natural character.

1) Essential BCs and ICs

With the magnetic vector potential formulation, BC (13a) when homogeneous, i.e. $\boldsymbol{n}\cdot\boldsymbol{b}_1|_{\gamma_1^+}=0$, leads to an essential BC on the primary unknown $\boldsymbol{a}_1$ that can be expressed in general (in 3-D) via the definition of a surface scalar potential u_1 [10], i.e.,

$$\boldsymbol{n}\cdot\operatorname{curl}\boldsymbol{a}_1\big|_{\gamma_1^+}=0\Leftrightarrow\boldsymbol{n}\times\boldsymbol{a}_1\big|_{\gamma_1^+}=\boldsymbol{n}\times\operatorname{grad}u_1\big|_{\gamma_1^+}\,. \tag{18}$$

This potential is multi-valued if a net magnetic flux flows in the domain Ω_1^+ bordered by γ_1^+. Its discontinuity through cut lines, making the boundary γ_1 simply connected, is directly related to the net flux. In 2-D, this BC amounts to define a floating magnetic vector potential $\boldsymbol{a}_1$ (with a constant perpendicular component) on each non-connected part of γ_1.

For problem 2, IC (16), when homogeneous, is simply treated with a continuous $\boldsymbol{a}_2$ through γ_2. When non-homogeneous, it can be expressed with a known discontinuous component $\boldsymbol{b}_{d,2}$ of $\boldsymbol{b}_2$ acting only in Ω_2^+, with $\boldsymbol{b}_2=\boldsymbol{b}_{c,2}+\boldsymbol{b}_{d,2}$, i.e.

$$[\boldsymbol{n}\cdot\boldsymbol{b}_2]_{\gamma_2}=\boldsymbol{n}\cdot\boldsymbol{b}_{d,2}|_{\gamma_2^+}=-\boldsymbol{n}\cdot\boldsymbol{b}_1|_{\gamma_1^+}\,, \tag{19}$$

or with an associated known discontinuous component $\boldsymbol{a}_{d,2}$ of $\boldsymbol{a}_2$, with $\boldsymbol{a}_2=\boldsymbol{a}_{c,2}+\boldsymbol{a}_{d,2}$, also acting only in Ω_2^+, i.e.

$$\boldsymbol{a}_{d,2}|_{\gamma_2^+}=-\boldsymbol{a}_1|_{\gamma_1^+}. \tag{20}$$

2) Natural BCs and ICs

With the magnetic vector potential formulation, an homogeneous BC (14a) is simply defined by zeroing the surface integral term related to $\gamma_1^+\subset\Gamma_{h,1}$ in (2), i.e. $<\boldsymbol{n}\times\boldsymbol{h}_1,\boldsymbol{a}'>_{\gamma_1^+}=<0,\boldsymbol{a}'>_{\gamma_1^+}=0$.

For problem 2, IC (17), when homogeneous, is treated similarly. When non-homogeneous, it has to act in a weak sense via the surface integral term related to γ_2 in (2). Indeed, the involved surface source $\boldsymbol{n}\times\boldsymbol{h}_1$ is only known in a weak sense on γ_2. One has, with (17) and (2) for $p=1$,

$$\begin{aligned}&<[\boldsymbol{n}\times\boldsymbol{h}_2]_{\gamma_2},\boldsymbol{a}'>_{\gamma_2}=<-\boldsymbol{n}\times\boldsymbol{h}_1,\boldsymbol{a}'>_{\gamma_2^+}\\&=<-\boldsymbol{n}\times\boldsymbol{h}_1,\boldsymbol{a}'>_{\gamma_1^+}=(\mu_1^{-1}\operatorname{curl}\boldsymbol{a}_1,\operatorname{curl}\boldsymbol{a}')_{\Omega_1^+=\Omega_2^+}\,.\end{aligned} \tag{21}$$

in case no part of $\Omega_{c,1}\setminus\Omega_1^+$ is in contact with γ_1^+ (otherwise the third term of (2) has to be considered as well). This way, the surface integral source term on γ_2 in (2) is calculated from a volume integral coming from the previous problem 1. Its consideration via a volume integral, limited at the discrete level to one single layer of FEs touching the boundary, is the natural way to average it as a weak quantity. Any other evaluation would not be consistent with the FE formulation used.

At the discrete level, the source quantity $\boldsymbol{a}_1$ in (21), given in mesh 1, has to be projected in mesh 2 via (3), with $\Omega_{s,p}$ limited to the layer of FEs touching γ_2^+. The test function $\boldsymbol{a}'$ in (21) is associated only with the edges of γ_2; the support of the function curl $\boldsymbol{a}'$ is indeed limited to this layer. This reduced support decreases the computational effort of the projection process.

B. Change from ideal to real flux tubes

A change of ICs is first applied to flux tubes. In a first problem $p=1$, the magnetic flux is forced to flow only in a subregion with perfect flux walls, i.e. a set of flux tubes $\Omega_1=\Omega_{ft,1}$ of the complete domain Ω. A second problem $p=2$ considers then the flux walls become permeable. This allows leakage flux in the exterior region $\Omega\setminus\Omega_1$ and leads to a change of the flux distribution in Ω_1. A solution refinement is thus achieved.

In problem 1, the ideal flux tubes are considered with a zero normal magnetic flux density BC on their boundaries $\Gamma_{ft,1}=\partial\Omega_1$, called flux walls. The trace of the magnetic field is unknown on $\Gamma_{ft,1}$. Once determined from the solution in Ω_1, it can be used as a BC to calculate the solution in $\Omega\setminus\Omega_1$, with all the precise characteristics of this exterior region (e.g., inductors and other surrounding regions). This task is however avoided, preferring the magnetic field to be simply zero in $\Omega\setminus\Omega_1$. With that purpose, problem 1 gathers all the inductor parts of the exterior region inside the double layer defined by $\Gamma_{ft,1}^+$ and $\Gamma_{ft,1}^-$, the inner and outer sides of $\Gamma_{ft,1}$ with regard to Ω_1 (Fig. 6, *left*). This defines idealized inductors and allows the magnetic field to be zero in $\Omega\setminus\Omega_1$. Each problem $p>1$ must then correct the already obtained solutions, in particular solution 1, via particular corrections of ICs (Fig. 6, *right*).

These constraints can be expressed in problem 1 via (13)-(15) with $\gamma_1=\Gamma_{ft,1}$, $\boldsymbol{b}_{su,1}=0$ and $\boldsymbol{j}_{su,1}$ unknown. Then, ICs (16)-(17) of problem 2 become

$$[\boldsymbol{n}\cdot\boldsymbol{b}_2]_{\Gamma_{ft,2}}=0\,,\quad [\boldsymbol{n}\times\boldsymbol{h}_2]_{\Gamma_{ft,2}}=-\boldsymbol{n}\times\boldsymbol{h}_1|_{\Gamma_{ft,1}^+}\,. \tag{22a-b}$$

Formulation $p=1$ is obtained from (2) with $\boldsymbol{b}_{s,1}=0$, $\boldsymbol{j}_{s,1}=0$,

$\boldsymbol{n}\times\boldsymbol{h}_{s,1}|_{\Gamma_{h,1}}=0$, $\gamma_1=\Gamma_{ft,1}\subset\Gamma_{b,1}$. The surface integral term $<\boldsymbol{n}\times\boldsymbol{h}_1,\boldsymbol{a}'>_{\Gamma_{ft,1}}$ is non-zero only for the test function $\boldsymbol{a}'=\text{grad}\,u'$ (from (18)), the value of which is then the MMF F_1 associated with a flux tube (for demonstration, see the general procedure developed in [10]). It is zero for all the other local test functions (at the discrete level, for any edge not belonging to $\Gamma_{ft,1}$). Therefore, the magnetic circuit relation can be expressed for each flux tube $\Omega_{ft,1}$, to relate fluxes and MMFs.

The correction formulation $p=2$ is then obtained from (2) with $\boldsymbol{b}_{s,2}=0$, $\boldsymbol{n}\times\boldsymbol{h}_{s,2}|_{\Gamma_{h,2}}=0$ and $\gamma_2=\Gamma_{ft,2}$. The volume source current density $\boldsymbol{j}_{s,2}$ is now defined in the inductor portions added to the studied domain Ω_2, in place of the firstly idealized inductors. IC (22a) is strongly expressed via the tangential continuity of the vector potential $\boldsymbol{a}_2$ through $\Gamma_{ft,2}$. IC (22b) is weakly expressed via (21).

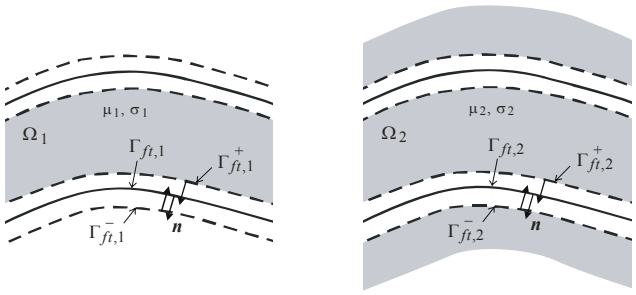

Fig. 6. Domains for the ideal (p=1, *left*) and real (p=2, *right*) flux tube problems.

A 2-D model of an electromagnet is considered as illustration. It consists of a U-shape core surrounded by a stranded inductor and separated from an I-shape core via two air gaps (Fig. 7) [9]. Both cores are 20 mm wide and deep. Their relative permeability is $\mu_{r,U\text{-}core}=\mu_{r,I\text{-}core}=500$. Each gap is 2 mm. An approximate solution $p=1$ is first calculated in an idealized flux tube (Fig. 8, $\boldsymbol{b}_1$), with a fixed MMF as excitation and a coarse mesh of the tube (Fig. 7, *middle*). This solution serves then as a source for a perturbation problem $p=2$ allowing leakage flux in the inner region of the core (Fig. 8, $\boldsymbol{b}_2$), followed by another problem $p=3$ allowing leakage flux in the outer region (Fig. 8, $\boldsymbol{b}_3$). Each problem calculates the actual flux distribution in the related inductor portion (the inner portion for problem 2 and the outer portion for problem 3) and in the vicinity of the gaps, with its own adapted mesh. They also correct the flux density in the cores. The magnetic flux density along the top surface of the I-core (entering the air gap) and through core portions is shown for the sequence of problems in Fig. 9. The corrections local to the gap region properly influence the inductor flux linkage, as pointed out in Fig. 9 (*bottom*). The approximate inductor flux linkage is $\Phi_1=108.8$ mWb and its corrections given by solutions 2 and 3 are $\Phi_2=33.8$ mWb and $\Phi_3=1.7$ mWb, i.e. 31 % and 1.6 % of the initial flux Φ_1 respectively.

The procedure could be extended to allow a 3-D distribution of the solution. The 2-D solution is first considered as limited to a certain thickness in the third dimension, with a zero field outside. Changes of ICs on each side of this portion should then allow the calculation of 3-D end effects. Considering the nonlinear behavior of the magnetic materials can define another perturbation problem.

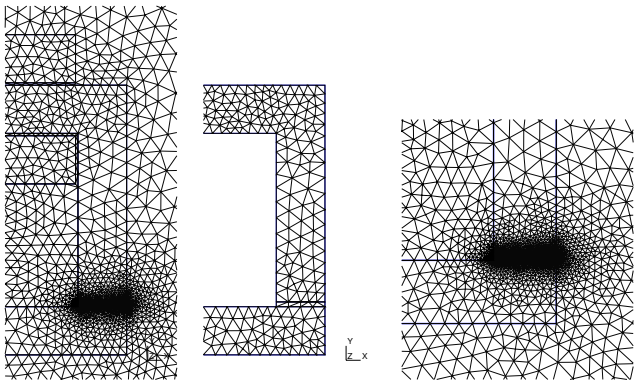

Fig. 7. Meshes (half portions) of the complete domain (*left*) and the ideal flux tube (*middle*); refined mesh in the vicinity of the air gap for a perturbation problem (*right*).

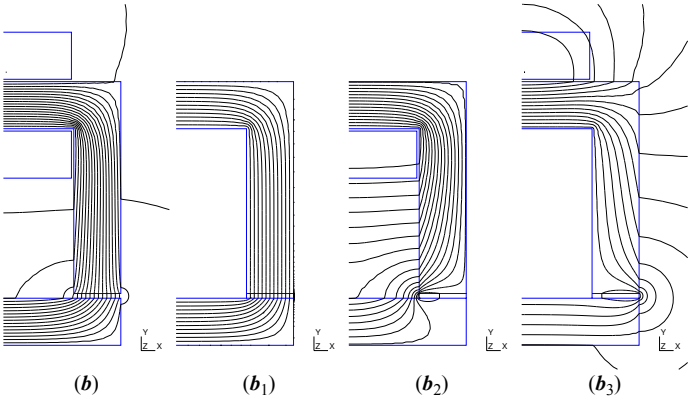

Fig. 8. Field lines of the complete solution ($\boldsymbol{b}$), in the ideal flux tube ($\boldsymbol{b}_1$) and in the perturbation problems with the inner ($\boldsymbol{b}_2$) and outer ($\boldsymbol{b}_3$) leakage fluxes (from left to right; the perturbation flux between two consecutive field lines is 4 times lower than for the source flux).

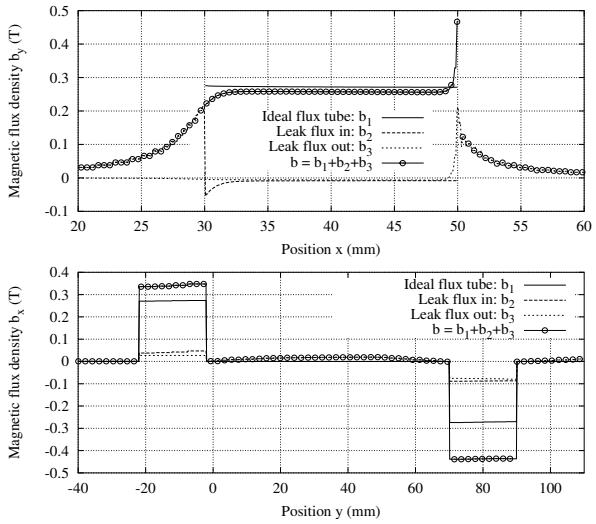

Fig. 9. Magnetic flux density along the top surface of the I-core (entering the air gap; *top*) and through the horizontal legs of the electromagnet (*bottom*) for the ideal flux tube ($\boldsymbol{b}_1$) and the inner ($\boldsymbol{b}_2$) and outer ($\boldsymbol{b}_3$) leakage fluxes; their addition gives the complete solution ($\boldsymbol{b}$).

C. Change from perfect to real conductive materials

A first problem considers perfect conductors, with $\sigma_1\to\infty$ (Fig. 10, *left*). These are denoted $\Omega_{cpe,1}\subset\Omega_{c,1}\subset\Omega_1$, and their boundary $\Gamma_{cpe,1}=\partial\Omega_{cpe,1}$. The resulting surface currents are considered to flow between the outer and inner sides of $\Gamma_{cpe,1}$ with regard to $\Omega_{cpe,1}$, i.e. $\Gamma_{cpe,1}{}^{+}$ and $\Gamma_{cpe,1}{}^{-}$. The perfect

conductors $\Omega_{cpe,1}$ are extracted from Ω_1 in (1) and treated via a BC of zero normal magnetic flux density on their boundaries $\Gamma_{cpe,1}{}^{+}$. The same BC occurs on $\Gamma_{cpe,1}{}^{-}$.

These constraints can be expressed in problem 1 via (13)-(15) with $\gamma_1 = \Gamma_{cpe,1}$, $\boldsymbol{b}_{su,1} = 0$ and $\boldsymbol{j}_{su,1}$ unknown. ICs (16)-(17) of problem 2 become

$$[\boldsymbol{n}\cdot\boldsymbol{b}_2]_{\Gamma_{cpe,2}} = 0\,, \quad [\boldsymbol{n}\times\boldsymbol{h}_2]_{\Gamma_{cpe,2}} = -\boldsymbol{n}\times\boldsymbol{h}_1|_{\Gamma_{cpe,1}{}^{+}}\,. \qquad \text{(23a-b)}$$

Formulation $p = 1$ is obtained from (2) with the perfect conductors extracted from Ω_1 and $\Omega_{c,1}$, and only involved through their boundaries $\gamma_1 = \Gamma_{cpe,1}$ with the homogeneous BC (13a). This latter condition is strongly defined in $F_1{}^1(\Omega_1)$. The boundary $\Gamma_{cpe,1}$ is thus added to $\Gamma_{b,1}$.

The surface integral term $<\boldsymbol{n}\times\boldsymbol{h}_1, \boldsymbol{a}'>_{\Gamma_{cpe,1}}$ is non-zero only for the function grad u' (from (18)), the value of which is then the total surface current I_1 flowing in $\Gamma_{cpe,1}$ [10]. It is zero for all the other local test functions (at the discrete level, for any edge not belonging to $\Gamma_{cpe,1}$). This way, the circuit relation can be expressed for each conductor $\Omega_{cpe,1}$ and the coupling with electrical circuits is possible.

For the correction formulation $p = 2$ (2), IC (23a) is strongly expressed via the tangential continuity of the vector potential $\boldsymbol{a}_2$ through $\Gamma_{cpe,2}$. IC (23b) is weakly expressed via (21).

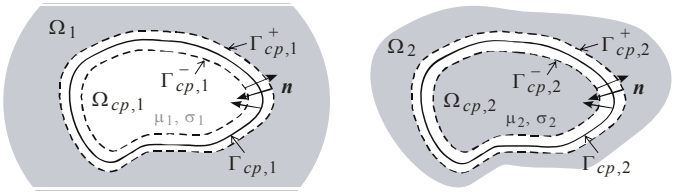

Fig. 10. Domains for the reference (*left*) and perturbation (*right*) problems, starting from perfectly electric ($cp \equiv cpe$) or magnetic conductors ($cp \equiv cpm$).

As illustration, a core-inductor system is considered (Fig. 11; five copper stranded inductors connected in series, aluminium core, 2-D model with vertical symmetry axis, frequency domain analysis at 5 kHz (skin depth $\delta = \delta_{Al} = 1.37$ mm), core half-width of 12.5 mm (9.1 δ) and height of 50 mm (36.5 δ)). Holes are considered in the core in order to point out the effect of corners. They are non-uniformly distributed to allow for different lengths of plane portions between them.

The magnetic flux lines are depicted in Fig. 11 for the different calculations performed, i.e. the conventional FE approach, the reference problem and the perturbation problem. Fig. 12 shows the eddy current and Joule power density distributions in the core, as well as the relative error on these quantities committed when using the impedance boundary condition (IBC) technique versus the subdomain FE approach (small lengths of plane portions penalize the IBC technique, which is based on analytical solutions valid far from any geometrical discontinuities, e.g. edges and corners). The results are checked to be very similar to those of the conventional FE approach. The error significantly increases in the vicinity of the conductor corners: it reaches 50% for the Joule power density and 30% for the current density in the smallest plane portions. This affects the total losses accuracy when the size of the conductor portions decreases. The error with the IBC is shown to be significant up to a distance of about 3 δ from each corner. A good accuracy is only obtained beyond this distance. The IBC error increases with δ with respect to the structure dimensions, whereas the developed approach successfully and accurately adapts its solution to any δ. The IBC solution could be also used to feed the ICs (16) and (17), both being thus non-homogeneous, of a perturbation problem.

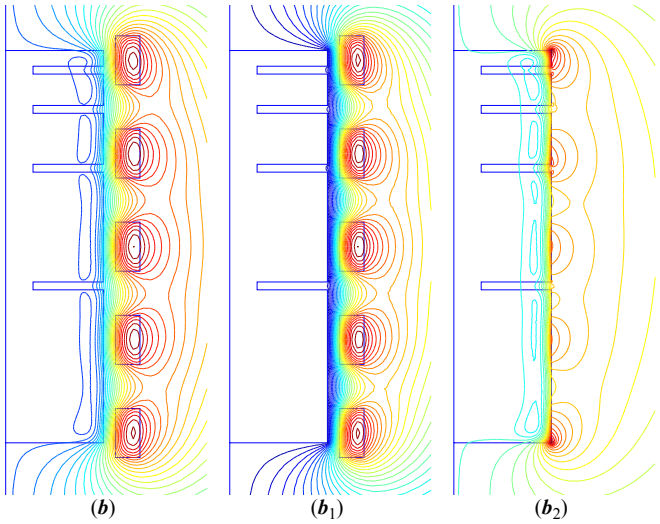

Fig. 11. Magnetic flux lines for the conventional FE solution $\boldsymbol{b}$, the reference solution $\boldsymbol{b}_1$ and the perturbation solution $\boldsymbol{b}_2$; system with a conductive non-magnetic core (aluminium) [8].

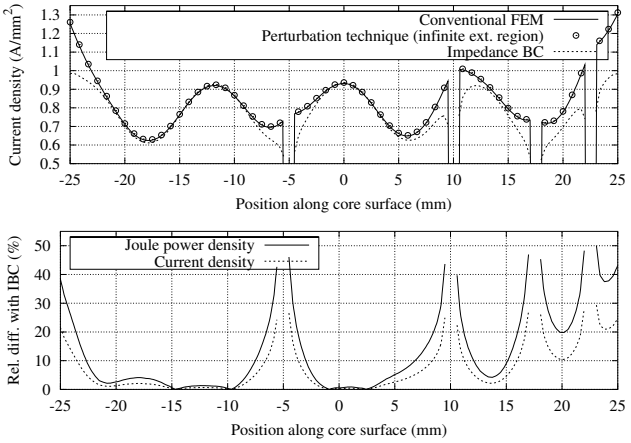

Fig. 12. Eddy current density along the core surface for the conventional FE solution, the perturbation technique and the IBC technique (*top*); relative difference between solutions of the last two techniques (*bottom*); system with a conductive non-magnetic core (aluminium) [8].

D. Change from perfect to real magnetic materials

Another reference problem considers conductors $\Omega_{cpm,1} \subset \Omega_{c,1} \subset \Omega_1$, of boundary $\Gamma_{cpm,1} = \partial\Omega_{cpm,1}$, as perfect magnetic materials, i.e. with $\mu_1 \to \infty$ (Fig. 10, *left*). The domain $\Omega_{cpm,1}$ can thus be extracted from Ω_1 in (1) and treated via a BC fixing a zero tangential magnetic field on its boundary $\Gamma_{cpm,1}{}^{+}$. Because only zero fields exist in $\Omega_{cpm,1}$, the same BC appear on $\Gamma_{cpm,1}{}^{-}$.

These constraints can be expressed in problem 1 via (13)-(15) with $\gamma_1 = \Gamma_{cpm,1}$, $\boldsymbol{b}_{su,1}$ unknown and $\boldsymbol{j}_{su,1} = 0$. Then, ICs (16)-(17) of problem 2 become

$$[\boldsymbol{n}\cdot\boldsymbol{b}_2]_{\Gamma_{cpm,2}} = -\boldsymbol{n}\cdot\boldsymbol{b}_1|_{\Gamma_{cpm,1}{}^{+}}\,, \quad [\boldsymbol{n}\times\boldsymbol{h}_2]_{\Gamma_{cpm,2}} = 0\,. \qquad \text{(24a-b)}$$

Formulation $p = 1$ is obtained from (2) with the perfect magnetic materials extracted from Ω_1 and $\Omega_{c,1}$ and only